

QUANTIFYING PHOTOVOLTAIC FIRE DANGER REDUCTION WITH ARC-FAULT CIRCUIT INTERRUPTERS

Kenneth M. Armijo*, Jay Johnson*, Richard K. Harrison*, Kara E. Thomas**, Michael Hibbs*, Armando Fresquez*

* Sandia National Laboratories
P.O. Box 5800
Albuquerque, NM 87185
kmarmij@sandia.gov
jjohns2@sandia.gov
rkharri@sandia.gov
mhibbs@sandia.gov
afresqu@sandia.gov

** The George Washington University
Department of Chemistry
725 21st Street NW
Washington, DC 20052
kethoma@sandia.gov

ABSTRACT: Unmitigated arc-faults present fire dangers, shock hazards, and cause system downtime in photovoltaic (PV) systems. The 2011 *National Electrical Code*® added section 690.11 to require a listed arc-fault protection device on new PV systems. Underwriters Laboratories created the outline of investigation for PV DC arc-fault circuit protection, UL 1699B, for certifying arc-fault circuit interrupters (AFCIs) for arc suppression. Unfortunately, little is known about appropriate trip times for arc-faults generated at different locations in the PV system, with different electrode and polymer encapsulant geometries and materials. In this investigation, a plasma model was developed which determines fire danger with UL 1699B-listed AFCIs and consequences of arc-fault discharges sustained beyond UL 1699B trip time requirements. This model predicts temperatures for varying system configurations and was validated by 100 and 300 W arc-faults experiments where combustion times and temperatures were measured. This investigation then extrapolated burn characteristics using this model to predict polymer ignition times for exposure to arc power levels between 100-1200 W. The numerical results indicate AFCI maximum trip times required by UL 1699B are sufficient to suppress 100-1200 W arc-faults prior to fire initiation. Optical emission spectroscopy and thermochemical decomposition analysis were also conducted to assess spectral and chemical degradation of the polymer sheath.

Keywords: Arc-Fault, PV Fire, Characterization, Modeling, Spectroscopy, Reliability

1 INTRODUCTION

Arc-faults have caused a number of PV installation and rooftop fires [1-4]. To address the hazards associated with PV arc-faults, the US *National Electrical Code*® (*NEC*) [5] has required arc-fault circuit interrupters (AFCIs), for PV systems greater than 80V, since 2011. Underwriters Laboratory (UL) has created a draft standard for listing AFCIs, UL 1699B, which requires AFCIs to detect arc-faults between 300-900 W within a certain amount of time. Each arc power in UL 1699B has a required AFCI trip time based on burn tests performed by Hastings, *et al.* [6] and independent studies by UL [7]. However, in previous studies at Sandia National Laboratories and utility-scale PV installations, arc-faults have been sustained well below these power values [8-9, 30]. As a result, Sandia National Laboratories provided recommendations to the UL 1699B Standards Technical Panel (STP) to include a low power arc-fault test at 100 W to ensure that AFCIs trip for low power arc-faults on single strings [8, 31-32]. It was believed that AFCIs located remotely topologically (e.g., at the inverter) may have more difficulty detecting low power arc-faults in large systems since the arcing signal-to-noise ratio would be smaller [30]. Many AFCIs use the DC spectral content to determine when there is an arc-fault [9-11], so lower power arc-faults—e.g., at the string level—will produce less conducted energy and the array current and voltage will not deviate for the original operating point as significantly during the fault. The experiments and analytical work contained in this paper seek to:

- a. Validate UL 1699B trip times are appropriate for 100-1200 W arc-faults based on polymer ignition time.

- b. Determine the fire danger with and without AFCIs by measuring and modeling transient temperatures of polymers in the proximity of the arc-fault.

In order to find appropriate AFCI trip times for newly proposed 100 W low power arc-faults, experimental and analytical analysis of arc-faults were conducted. PV fires are caused by the high-temperature plasma associated with an arc-fault, so transient simulations of low power arcs were conducted to determine plasma, anode and cathode, and surrounding polymer temperatures. The simulations were calibrated with experimental tests using the UL 1699B test setup with thermocouples placed at the anode, cathode, and polymer tube [31, 32]. Burn times for a polycarbonate material was predicted based on conduction within the test setup and combustion temperatures. It is believed here that other polymers common to PV systems, such as Tedlar® (PVF) would also behave similar to one these materials, however future research is needed to validate this hypothesis.

Experimental and analytical investigations of DC-DC plasma discharges are almost entirely restricted to simplified geometries and non-air environments. This is due to the reaction complexity within air plasmas and their respective material boundary conditions [12]. Very high temperatures are typically needed to sustain ionization, which is a defining feature of DC-DC discharge plasma. The degree of plasma ionization is determined by its respective 'electron temperature' relative to the present system ionization energy, which is heavily influenced by the presence of oxygen, material boundary conditions, and electrode gap spacing and geometry.

To date, although analytical models exist for 1 atm

plasmas [12, 28] in non-PV applications, virtually no models exist that characterize DC-DC discharge plasmas for PV arc-faults, especially with an air medium. This may be due to the complexity in characterizing this specific type of discharge, and difficulty in experimental validation. However, prior welding research by Lowke [18], among other investigators [17, 29] with differing geometrical constraints, have provided constitutive analytical formulations for DC-DC discharge plasmas, which have been adopted for this work.

To corroborate the analytical calculations, residues of polymer samples exposed to arcs were measured with IR spectroscopy to determine the degree of their respective thermal decomposition. The samples were of varying materials/geometries and were exposed to different arc-power levels. The geometry was varied to allow for the replenishment of oxygen, simulating an arc-fault open to the atmosphere versus an arc-fault contained in the module, connector, or other self-contained areas within the array.

2. PHYSICS-BASED ARC-FAULT SIMULATIONS

A numerical model of a DC-DC discharge plasma arc-event was performed using MATLAB[®]. Fig. 1 shows the model domain used for computing the temperature fields within the plasma space and adjacent electrodes and polymer sheath components. For simplicity, only the plasma region and half of the cross section was considered due to symmetry.

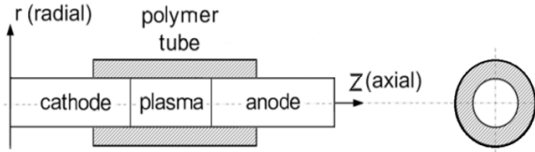


Fig. 1. MATLAB Plasma Arc Modeling Domain.

Under atmospheric pressure conditions, DC discharge plasma is generally collision dominated [13], whereby the mean free paths for all reaction species are much smaller than the macroscopic characteristic lengths [14]. Therefore, the plasma can be viewed as a continuum fluid described by mixture balance equations, obtained by summing over the equations of all individual species [14]. For this investigation, a 2D energy balance equation based on radial and axial temperatures was considered. To model the temperature distribution across the plasma and polymer sheath regions, a 2D finite difference method was employed using an implicit cylindrical coordinates discretization scheme, where the arc column was approximated to be axially centered, with a 1 mm diameter based on experimental observations. The gap spacing for this model was set at 5 mm with natural convection and radiation boundary conditions imposed on the outer surface of the polycarbonate sheath.

$$\frac{1}{r} \frac{\partial}{\partial r} \left(kr \frac{\partial T}{\partial r} \right) + \frac{\partial}{\partial z} \left(k \frac{\partial T}{\partial z} \right) + \dot{Q}_{plasma} = \rho C_p \frac{\partial T}{\partial t} \quad (1)$$

In Eqn. 1, the temperature, T , is calculated based on the plasma density, ρ , specific heat capacity, C_p , and thermal conductivity in W/m-K, k , which were determined from virial equations for air plasmas [15, 16]. Within the gas space (Fig. 1), the plasma heat transfer rate, \dot{Q}_{plasma} , includes Ohmic heating due to electron and ion currents, as well as losses due to radiation. The cumulative value is illustrated by,

$$\dot{Q}_{plasma} = jE - U(T) \quad (2)$$

where E is the electric field, j is the current density, and $U(T)$ is the radiation loss. For this study six power levels between 100-1200 W were analyzed, with current levels below 15 A. For low current plasmas, previous studies [17, 18] of atmospheric discharges in air found that radiation losses from the arc column were generally small for currents less than approximately 30 A. An investigation by Lowke *et al.* [17] was able to find agreement with their experiments when they omitted the radiation loss term from their model, which was found to be relatively negligible.

For this investigation, plasma thermodynamic equilibrium conditions were assumed with the approximation of homogeneous thermodynamic properties. Additional approximations include those provided by Lowke *et al.* [17] for low current arcs less than 10 A with negligible radial pressure gradients, as well as viscous and turbulence effects. The investigators also neglected electrode effects since the properties of the arc column were insensitive to electrode boundary conditions.

From Ohm's law, the electric field can be described by Eqn. 3, where σ is the electrical conductivity and A the cross-sectional area. From preliminary imaging analysis of several plasma columns at 100 W and 300 W power levels, the cross-sectional areas were observed here to have uniform diameters between the two electrodes. Therefore electron densities and respective electrical conductivity were approximated to be high and uniform throughout the axially-centered column, with negligibly low values throughout the rest of the air-space medium.

$$E = \frac{\partial V}{\partial z} = \frac{I}{\sigma A} \quad (3)$$

At the cathode/plasma interface, special treatment is required to account for cooling by the thermionic emission of electrons and heating by ion bombardment of the electrode [19]. Therefore at this interface the additional energy flux provided by Eqn. 4 is included in Eqn. 1, where

$$F = j_i V_i + j_e \left(\phi_w + \frac{2k_b T}{e} \right) \quad (4)$$

where ϕ_w is the work function of the cathode material, V_i is the ionization potential of the gas, k_b is the Stefan-Boltzmann constant, j_i is the ion current density, and j_e is the electron current density due to thermionic emission. At the anode/plasma interface Eqn. 4 is set to:

$$F = j_e \phi_w \quad (5)$$

where the ion current density is approximated to be zero and j_e is positive as electrons at this location are absorbed at the anode.

The theoretical thermionic current is provided by the Richardson equation where ξ is a measured material constant [20].

$$j_{rich} = \xi T^2 e^{\frac{-\phi_e}{k_b T}} \quad (6)$$

Since the imposed current densities j were larger than the theoretical current for thermionic emission [20], j_{rich} we assume here that at the cathode/plasma interface the excess current is carried by the ions where $j_i = j - j_{rich}$. In Eqn. 4, j_e accounts for thermionic cooling by electrons overcoming the work function by removing energy as they leave the cathode [17]. At this interface j_e is calculated

TABLE 1.

SUMMARY OF ARC-FAULT EXPERIMENTS WITH PV SIMULATOR AND ARC-FAULT GENERATOR IN A POLYCARBONATE SHEATH [31]

Test Number	Arc Power	Electrode Diameter	Electrode Tip	Hole	Avg. Fire Ignition Time [Sec.]	Standard Deviation Fire Ignition Time [Sec.]
1 (UL 1699B)	300 W	1/4"	Flat	No	14.6	10.7
2	300 W	1/4"	Flat	Yes	11.8	5.9
3	300 W	1/4"	Flat	No	14.1	9.0
4	100 W	1/4"	Flat	No	69.0	41.1
5	100 W	1/4"	Flat	Yes	22.0	12.7
6	100 W	1/4"	Round	Yes	107.0	17.0
7	100 W	1/8"	Flat	Yes	21.7	4.5
8	300 W	1/8"	Flat	Yes	10.3	4.0

based on the expression provided by Morrow and Lowke [17] where j_i for a uniform discharge is negative, whereas j_e and E are positive. Further details for the determination of j_i and j_e can also be found in their work.

$$j = j_e - j_i \quad (7)$$

By solving Eqn. 1 with an implicit numerical scheme [34] using Eqns. 2-7 as inputs, the respective transient thermal distributions through the media were determined.

3. ARC-FAULT EXPERIMENTATION

3.1 Electrical Testing Setup

A PV simulator at Sandia National Laboratories was developed to represent constant power I-V curves from a set of 1024 points, shown in Fig. 2. From experimental observations, the arc power was nearly constant for any given curve regardless of the electrode gap spacing. As a safety precaution, the PV simulator power was provided to the arc-fault generator through a power resistor so the simulator was never shorted. Additionally, the curves programmed into the PV simulator were limited to 600 V and 15 A.

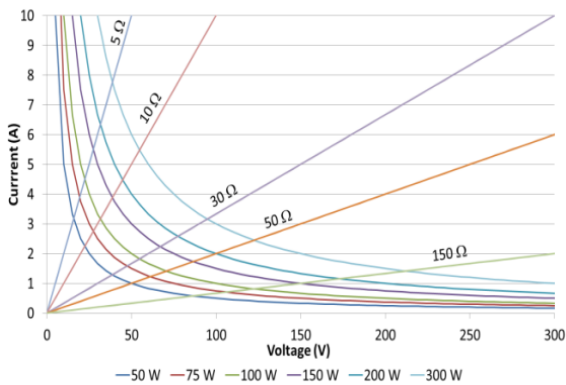


Fig. 2. Constant Power Arc-Fault IV Simulation Test Curves.

In the experimental investigation, 100 W and 300 W constant power curves were evaluated [31, 32]. The list of arc-fault tests is shown in Table 1. Each test was performed at least 5 times to determine fire ignition times as well as to evaluate the ease of initiating and sustaining an arc [31].

As shown in Fig. 3, the experimental setup used in this investigation consists of an arc-fault generator, with current and voltage probes, as well as a k-type thermocouple, which was placed on each respective polymer test sheath.

For test purposes, each annular test piece (sheath), with a 0.125 inch wall thickness, 0.75 inch length, and 0.25 inch internal diameter was inserted over the two electrodes. For this apparatus, the electrodes—one moveable (anode) and one stationary (cathode)—were made of solid copper. The electrodes were separated using a lateral adjustment of the moveable electrode to the desired gap spacing.

In addition, a set of test specimens were machined with a small centralized hole to assess combustion rates with an increased presence of oxygen. The hole simulated an arc-fault open to the atmosphere versus an arc-fault contained in the module, connector, or other self-contained area within the array. The polymer specimens were placed halfway over the stationary electrode and the moveable electrode was then adjusted to the appropriate gap distance from the stationary electrode. During each test, PV power was applied until the sample pyrolyzed by setting the electrode gap appropriately to sustain the arc. A UL-listed smoke detector was also installed just above the arc-fault generator and high-speed video recordings were collected to determine the first instance of smoke and subsequent combustion of the sheath material.

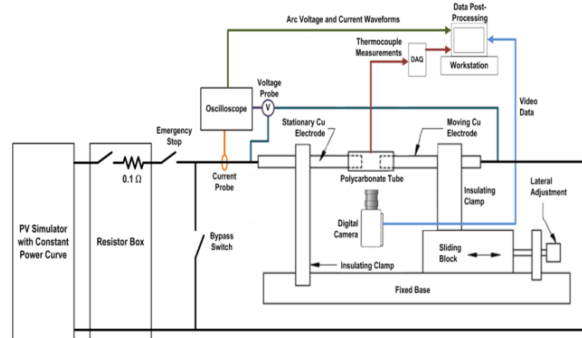


Fig. 3. Experimental configuration and data acquisition system.

3.2 Degradation of Polymers with Plasma Exposure

More than 100 parameterized arc-fault experiments were performed using the test system. The experimental results can be seen in Fig. 4 for a 100 W arc with a 0.25 inch diameter polycarbonate sheath, containing a 0.25 inch hole for air ingress. The data indicates steadily increasing temperatures as the polycarbonate sheath reacts to the DC-DC discharge plasma arc.

The arc-fault videos obtained from the digital camera were converted into a series of frames so the time to polymer melting, smoke formation, and fire were either validated or determined from measurements (i.e.

thermocouples and smoke detector). In most of the 100 W arc-fault tests the time to reach smoke and fire combustion was greater than 20 seconds. While a small number of tests did not reach the fire ignition point, it was clear that 100 W arc-faults are capable of causing fires in PV systems. Additional parametric results for other tests can be found in Armijo *et al.* [31].

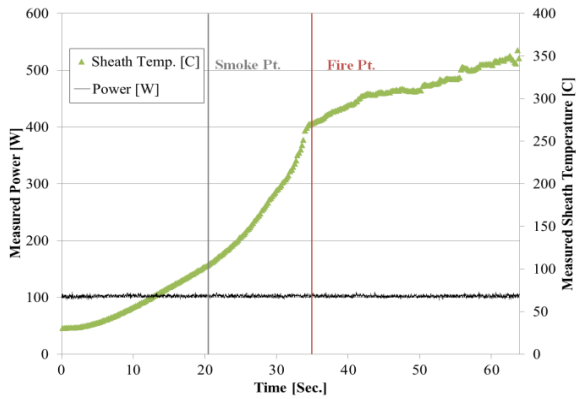


Fig. 4. 100 W arc-fault test results using a 0.25 inch diameter polycarbonate sheath that includes a 0.125 inch hole. The arc-fault was established at time = 0 s.

For the tests with polycarbonate sheaths, the average time to detect smoke was 9.4 s with a minimum value of 2.5 s, while the average time to detect fire combustion was 33.8 s. In situations where the polymer did not combust, the sheath and electrodes heated up to the point that the sheath melted off the hot electrodes.

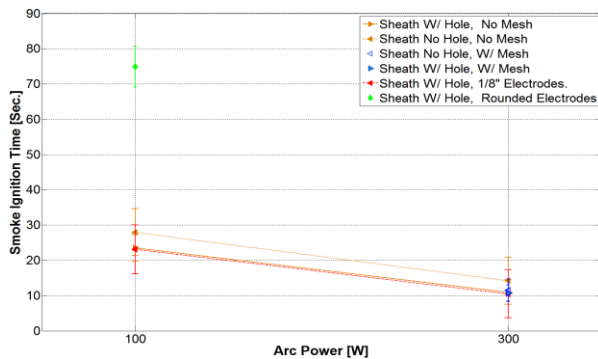


Fig. 5. Parametric arc-fault tests using 0.125 inch and 0.25 inch diameter copper electrodes, for 100 W and 300 W arc discharges, with and without oxidation holes and arc initiation wire mesh.

The results in Fig. 5 indicate that a difference of 1.7% and 4.7% in smoke ignition times between electrode diameters of 0.25 inches and 0.125 inches, for respective 100 W and 300 W power levels. Reducing the electrode diameter constrains the air volume for plasma discharge, which impacts off-gas concentrations of reactive species, surface chemical reactivity [22], as well as the respective ionization potential [23] to initiate the arc.

Additionally, the inclusion of a small centrally-located 0.125 inch hole suggested improved arc sustainability for both 100 W and 300 W power levels. The results showed a 16.1% and 22.9% decrease in ignition times for the respective 100 W and 300 W polycarbonate tests with the inclusion of the hole. Previous research by Pandiyaraj *et al.* [24] also found increased oxygen levels increased plasma/surface interfacial

chemical potentials, which influence ionization potentials and the capability for ignition [25].

The rounded-tip electrodes improved arc stability since the plasma stream remained centered at the minimum electrode gap distance, rather than exhibiting radial movement as in the case with the flat-surface electrodes. This effect was associated with an increase in the visible ignition time by as much as 35.5%. It was postulated that the rounded-tip electrodes constrain the arc plasma stream to the radial center of the electrode cavity, reducing contact between the polymer and the plasma stream. These types of electrodes were found to cause more uniform heating of the polymer material, which would eventually melt into the arc gap and ignite.

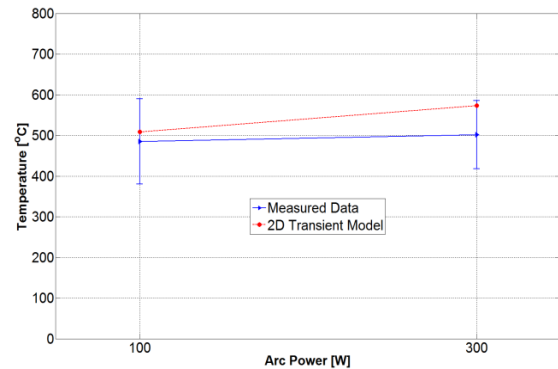


Fig. 6. Outer polycarbonate sheath temperature comparison between simulated and the average of the measured data for 100 and 300 W arc-faults after the average arc-extinguish time period.

Analysis of the transient 2D model revealed good agreement with experimental data with a uniform polycarbonate sheath, without the inclusion of a hole or arc ignition mesh. The 100 W input power-level exhibited a 4.9% uncertainty and the 300 W case had 14.2% uncertainty after 69 s which was the average arc-extinguish time period.

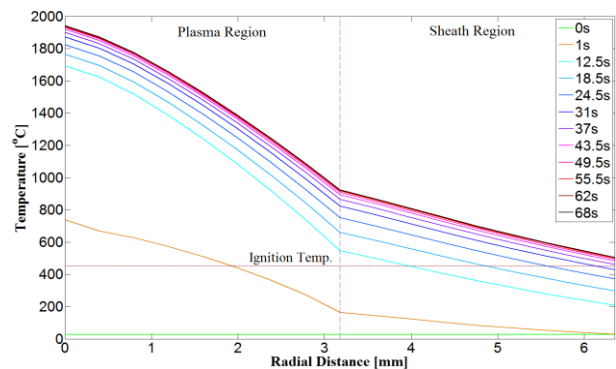


Fig. 7. Simulated plasma and polycarbonate sheath region temperatures for a 100 W input power level, within air ambient conditions and a pressure of 1 atm.

Due to the approximation of a constant electric field across the electrode gap, average low temperature variations of 0.87% and 0.68% were found across the respective plasma and sheath regions. However, larger radial variations were found, where average temperatures of 788.7°C and 346.7°C were observed across the plasma and sheath regions respectively.

In this analysis the time duration of the simulation was

TABLE 2.

MODEL PREDICTED TRANSIENT POLYCARBONATE MATERIAL TEMPERATURES [°C] FOR POWER LEVELS BETWEEN 100-1200 W.

Arc Power [W]	Arc Duration Time [sec.]										
	0.20	0.40	0.63	0.83	1.15	1.50	2.00	4.00	6.00	8.00	10.00
100	25.79	27.03	33.06	41.94	61.23	86.90	128.03	297.40	425.27	499.96	538.53
300	25.91	28.87	40.87	58.66	98.42	153.16	242.46	556.19	694.35	743.50	760.65
500	26.05	30.78	49.15	76.87	140.46	229.68	372.76	754.14	861.42	890.81	898.93
650	26.13	32.00	54.49	88.81	168.60	280.93	455.90	846.23	936.74	958.79	964.23
900	26.27	33.99	63.38	108.97	216.57	367.08	584.86	961.27	1031.54	1046.20	1049.29
1200	26.44	36.37	74.23	133.93	276.20	470.04	719.73	1062.64	1116.78	1126.49	1128.25

Material Under Non-Destructive State
Material Undergoing Melting
Material Undergoing Fire Ignition

— UL 1699B AFCI Maximum Trip Time

$T_{\text{melt}} = 155^{\circ}\text{C}$

$T_{\text{ignition}} = 450^{\circ}\text{C}$

based on respective experimentally recorded times. Overall in an unmitigated arc-fault, without an AFCI device, the results indicate a significant danger as the predicted outer sheath temperatures can rise above the polycarbonate auto-ignition temperature of 450°C [27]. The model suggests that these temperatures can be as high as 508.96°C after approximately 60 s for a low 100 W power level. Experimental observations confirm the polymer fires after this time period, and in some cases much quicker if the interior polymer material melted into the plasma stream.

After validating the model with the experimental data from the 100 and 300 W arc-faults, the simulation was used to predict the burn times for higher power arc-faults. These arc-faults may occur on the output circuits of PV systems either after the combiner or recombiner box where currents can be between 15 and 500+ amps. In these locations, if there is a failure in the conductor or connector, either an arc flash will explosively damage the faulted region or—for lower currents—a sustained arc-fault will occur. UL 1699B only requires tests from 300-900 W, but the model was used to more broadly predict fire risk for 100–1200 W arc-faults. To evaluate this risk, the outer sheath temperature was calculated and compared to the ignition temperature for polycarbonate. The temperatures shown in Table 2, are the average (bulk) polymer temperature, which is the median radial temperature through the sheath. As the arc power increases there is less time before the polymer reaches the ignition temperature. Also, these results suggest increasing arc-power levels can have impacts on ignition time scales, which requires rapid and accurate AFCI responses. UL 1699B defines the maximum AFCI trip time according to Eqn. 7.

$$t_{\text{trip}} = \min\left(2, \frac{750}{i_{\text{arc}} V_{\text{arc}}}\right) \quad (7)$$

These trip times have been included in the table to determine polymer temperatures at the point when AFCIs must de-energize the arc-fault. As can be seen in the table, the trip times are sufficient to prevent the combustion of polycarbonate. The burn times of other PV polymer materials will differ based on their heat transfer properties and ignition temperature. If the AFCI fails to trip within the required period, the temperature of the polymer quickly reaches the combustion point so it is critical for these devices to effectively detect and mitigate the arc-fault.

4. OPTICAL EMISSION SPECTRUM ANALYSIS

To further validate the model, understand the plasma discharge process, and predict material degradation

mechanisms, measurements of the plasma electron temperature are necessary. Recent work indicates the optical emission spectrum of plasmas can be analyzed to calculate the electron plasma temperature [33]. This analysis will be used to develop a method to validate the electron temperature of the plasma as well as the plasma thermal model. For this study, optical spectra of the arc plasma were acquired using an Ocean Optics S2000 fiber spectrometer, which consisted of an integrated linear silicon CCD array and miniaturized optical bench. The spectrometer had a resolution of 0.33 nm, and a spectral measurement range of 340-1019 nm. The plasma spectra were optically coupled to the spectrometer using a diffusive cosine corrector free-space to fiber adapter. The position of the detector was adjusted relative to the arc to avoid saturation. A spectrum integration time of 100 ms was used, with a series of over 100 spectra captured per arc discharge trial to examine the change in emission and plasma conditions as a function of time.

Spectra were analyzed for 100 W and 300 W arcs using a polycarbonate sheath with and without a hole. From Fig. 8 the optical spectra for both arc discharge power levels correspond to atomic emission lines from singly ionized copper ions, which emanate from the electrodes. However, further study is needed to validate the degree of ionization and dissociation of ions in the plasma, which could affect the temperatures and optical emission for varying plasma conditions.

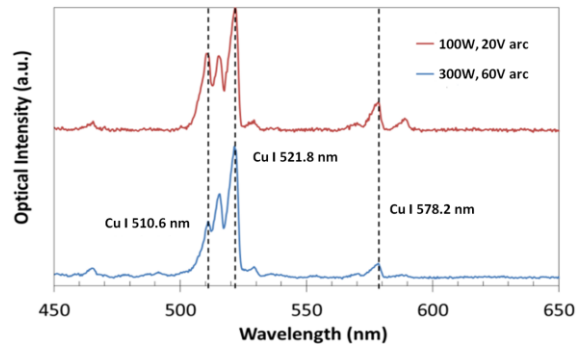


Fig. 8. Optical intensity emission spectra analysis for 100 W and 300 W arc power levels.

Changes in the emission line ratios were observed for the 522, 515 and 511 nm peaks between the two electrical power levels. It is postulated that these changes could correspond to differences in the plasma equilibrium and mean excitation levels of the copper ions, as would be expected for different excitation voltages that were employed, which were 20 and 60 V respectively.

An examination of the plasma emission for the 100 W power level as a function of time was also performed, with the results shown in Fig. 9. The chronological spectrum numbers contain information for 100 ms epochs. Interestingly, the emission line ratios provide a clear indication of arc discharge characteristics. For the 300 W case, the emission line ratios were roughly constant as a function of time during the arc. During the 100 W arc discharge increases of 24% and 30% were observed for the 511/522 and 511/515 ratios, respectively. These increases indicate rising plasma temperatures as a function of time, but further investigations are needed for quantitative analysis.

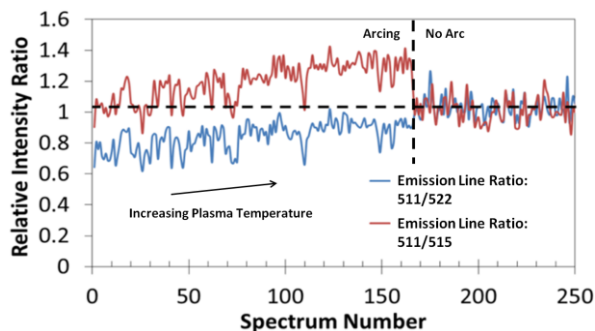


Fig. 9. Emission line ratio analysis for a 100 W arc power level, with emission line ratios evaluated for 511 nm/522 nm and 511 nm/515 nm peak pairs.

An examination of the plasma emission for the 100 W power level as a function of time was also performed, with the results shown in Fig. 9 provided as a spectrum number in the sequence of acquisition. Interestingly, the emission line ratios identified provide a clear indication of arc discharge by their correlation. For the 300 W case, the emission line ratios were roughly constant as a function of time during the arc. During the 100 W arc discharge increases of 24% and 30% were observed for the 511/522 and 511/515 ratios, respectively. These increases suggest potential rise in plasma temperatures as a function of time, however further investigation is needed for thermal validation.

The detected emission lines correspond to singly ionized copper ions in the arc column, but further testing and analysis will be needed to evaluate the degree of dissociation and ion excitation, which can impact the plasma composition and temperature.

During these tests, the acquisition of optical spectra was stopped after the arc self-extinguished. The extinction of the arc is clearly seen in the data when the emission line ratios fall to random correlation oscillating around one corresponding to the background electrical and optical noise.

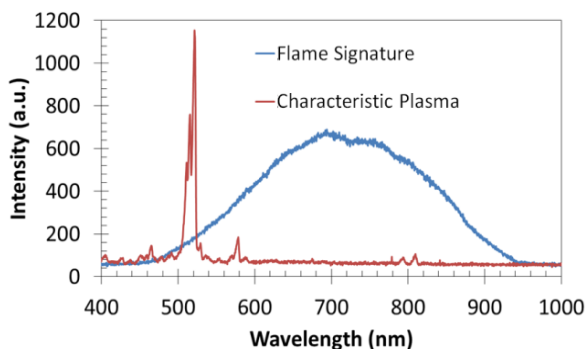


Fig. 10. Optical intensity emission spectra analysis for 100 and 300 W arc-faults.

Finally, optical emission spectra were compared for the 300W arc discharge of copper electrodes surrounded by a sheath with and without a hole, shown in Fig. 10. For the arc discharge utilizing a continuous sheath, optical emission corresponding to a flame signature was observed after the arc was extinguished and when the fire ignition point was reached. Here, we see a dramatic difference between characteristic plasma emission from the sheath containing a hole (red line), and the blackbody optical emission corresponding to the burning plastic sheath (blue line). These signals could provide an additional metric for identifying the onset of arc discharge or fire.

For the arc discharge utilizing a continuous sheath, optical emission corresponding to a flame signature was observed after the arc was extinguished and when the fire ignition point was reached. Here, we see a dramatic difference between characteristic plasma emission from the sheath containing a hole (red line), and the blackbody optical emission corresponding to the burning plastic sheath (blue line). These signals could provide an additional metric for identifying the onset of arc discharge or fire.

5. CHEMICAL DEGRADATION ANALYSIS

To further understand the degradation mechanisms of the varying polycarbonate geometries exposed to the arc plasma, the samples were cut open and subjected to Attenuated Total Reflection Fourier Transform Infrared Spectroscopy (ATR FTIR) analysis.

ATR FTIR experimental results of the polycarbonate samples exposed to arc-faults each showed markers in the IR spectra, identified as indicators of thermal polymer decomposition. These markers were specific peaks in the spectra that either corresponded to a reduction of a functional group in the control polymer (unburned sheath), or the appearance of new functional groups found in well-established decomposition products.

IR spectra were taken at several spatial positions on the samples with varying discoloration in order to determine the extent of the thermal oxidation reactions. Fig. 11 shows IR spectra from an unburned polycarbonate control sample and a polycarbonate sample exposed to an arc-fault. The two most obvious changes in these samples are:

1. The appearance of a broad peak between 3100 and 3500 cm^{-1} .
2. The diminishment of the sharp peak at 1772 cm^{-1} .

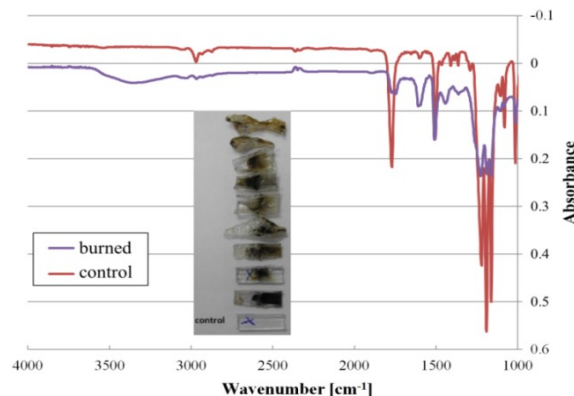


Fig. 11. IR spectral analysis of polycarbonate (PC) experimental and control sheaths.

The former is indicative of O-H stretching and the latter is due to reduced C=O stretching in a carbonate group. Both of these peaks are consistent with the decomposition reactions illustrated in Fig. 12. In the top reaction, polycarbonate was oxidized to give a phenol and a methyl ketone as products. In the bottom reaction, polycarbonate undergoes a loss of carbon dioxide to give an aryl ether product [26].

This chemical analysis shows that oxidation reactions (combustion) occur during the arc fault tests and changes in the appearance of the polymers are not only from melting. From Fig. 10, it is postulated that excess air enabled a fast, hot burn, while the closed-sheath tests ignited much slower. The products formed from the faster burn time typically had a more narrow range of products than if the combustion took place over a longer period of time. Therefore, extra oxygen would provide a different reaction pathway from a closed-sheath. These results indicate two of these potential degradation pathways the polycarbonate sheaths may have undergone during testing which may explain the optical emission differences in signatures.

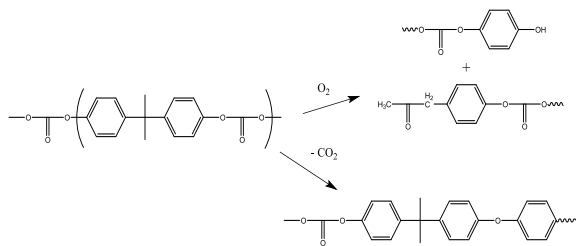


Fig. 12. Thermal decomposition pathways for polycarbonate.

6. CONCLUSIONS

PV arc-faults can damage the system and surrounding structures through quick ignition of polymer materials commonly used in PV systems. Underwriters Laboratories arc-fault circuit interrupter (AFCI) certification standard UL 1699B, lists required trip times for AFCI devices for the U.S. market. To determine if these trip levels were appropriate for fire mitigation experimental and numerical experiments were run for different arc-fault power levels. The results for both, indicate that polycarbonate will not combust prior to the AFCI maximum trip times required by UL 1699B.

The arc-fault plasma discharge model was also developed using a transient 2D finite difference method approach. The model was validated with experimental data for a uniform polycarbonate sheath with a 4.9% and 14.2% error for the 100 and 300 W power levels respectively. The numerical simulations indicated the necessity of including an AFCI within a PV system because an unmitigated arc will quickly produce sheath temperatures above PV polycarbonate ignition temperatures. Further research is ongoing to analyze the accuracy of this model with other PV materials and geometries.

The initial investigations show that optical emission spectroscopy is potentially useful for arc discharge characterization. Information obtained using this approach include optical emission as an indicator of arc formation, elemental analysis from characteristic emission lines, and an optical signature of flame. Further research into this promising technique will evaluate the use of spectroscopy to determine plasma temperatures and quantitative elemental compositions.

Finally based on fire ignition times and the 2.5 second minimum smoke detection time, it is suggested UL 1699B include a two second trip time requirement for 100 W arcs to

ensure the AFCIs can detect low power arc-faults and the AFCI certification standard provides a sufficient safety factor to ensure the arc is de-energized prior to any fire.

7. ACKNOWLEDGEMENT

Sandia National Laboratories is a multi-program laboratory managed and operated by Sandia Corporation, a wholly owned subsidiary of Lockheed Martin Corporation, for the U.S. Department of Energy's National Nuclear Security Administration under contract DE-AC04-94AL85000. This work was primarily funded by the US Department of Energy Solar Energy Technologies Program. This material is also based upon work partially supported by the U.S. Department of Homeland Security under Grant Award Numbers 2012-DN-130-NF0001-0202 and HSHQDC12X00059. The views and conclusions contained in this document are those of the authors and should not be interpreted as representing the official policies, either expressed or implied, of the U.S. Department of Homeland Security. The authors would also like to acknowledge fundamental contributions from Dr. Kenneth Williamson who is a plasma physics expert at Sandia National Laboratories.

8. REFERENCES

- [1] H. Laukamp, "Statistische Schadensanalyse an deutschen PV-Anlagen," PV Brandsicherheit workshop, Köln, Germany, Jan. 26th, 2012 (in German).
- [2] H. Schmidt, F. Reil, "Welcome to the 2nd Workshop 'PV Fire'," PV Brandsicherheit Workshop, Freiburg, Jan 2013 (in German).
- [3] C.C. Grant, Fire Fighter Safety and Emergency Response for Solar Power Systems, Fire Protection Research Foundation, May 2010.
- [4] L. Ji, "PV Fire: Experience and Studies," Photovoltaic Reliability Workshop II, Tempe, AZ, 31 July, 2009.
- [5] National Electrical Code, 2011 Edition, NFPA70, National Fire Protection Association, Quincy, MA.
- [6] J.K. Hastings, M.A. Juds, C.J. Luebke and B. Pahl, "A Study of Ignition Time for Materials Exposed to DC Arcing in PV Systems," 37th Photovoltaic Specialists Conference, Seattle, WA, 19-24 June 2011.
- [7] D.A. Dini and P.W. Brazis, "DC Arc Fault Testing to Support Photovoltaic Arc Fault Protection Device Requirements," UL Technical Document, Oct. 8th, 2013.
- [8] J. Johnson, "Suggestions for UL 1699B based on Arc-fault Testing at Sandia National Laboratories," private memo to UL 1699B Standards Technical Panel, 31 July 2012.
- [9] J. Johnson, B. Pahl, C.J. Luebke, T. Pier, T. Miller, J. Strauch, S. Kuszmaul and W. Bower, "Photovoltaic DC arc fault detector testing at Sandia National Laboratories," 37th IEEE PVSC, Seattle, WA, 19-24 June 2011.
- [10] J. Johnson, M. Montoya, S. McCalmont, G. Katzir, F. Fuks, J. Earle, A. Fresquez, S. Gonzalez, and J. Granata, "Differentiating series and parallel photovoltaic arc-faults," 38th IEEE PVSC, Austin, TX, 4 June, 2012.

- [11] J. Johnson, "Arc-fault detection and mitigation in PV systems: Industry progress and future needs," NREL Module Reliability Workshop, Denver, CO, 28 Feb. 2012.
- [12] E. Pfender, "Heat transfer from thermal plasmas to neighboring walls or electrodes," *Pe & Appl. Chem.*, 1976, **48**, pp. 199-213.
- [13] A. Fridman, "Plasma Chemistry," Cambridge Univ. Press, New York, NY, 2008.
- [14] K.H. Becker, U. Kogelschatz, K.H. Schoenbach and R.J. Barker, "Non-equilibrium air plasmas at atmospheric pressure," IOP Publishing Ltd, London, UK, 2005.
- [15] M. Capitelli, G. Colonna, C. Gorse, and A. D'Angola, "Transport properties of high temperature air in local thermodynamic equilibrium," *Eur. Phys. J.D.*, **11**, pp. 279-289, 2000.
- [16] A.B. Murphey, "Transport coefficients of air, argon-air, nitrogen-air, and oxygen-air plasmas," *Plasma Chemistry and Plasma Processing*, **15**, No. 2, pp. 279-307, 1995.
- [17] R. Marrow and J.J. Lowke, "A one-dimensional theory for the electrode sheaths of electric arc," *J. Phys. D: Appl. Phys.*, **26**, pp.634-642, 1993.
- [18] J.J. Lowke, "Simple theory of free-burning arcs," *J. Phys. D: Appl. Phys.*, **12**, pp. 1873-1886, 1979.
- [19] P. Zhu, J.J. Lowke, and R. Morrow, "A unified theory of free burning arcs, cathode sheaths and cathodes," *J. Phys. D: Appl. Phys.*, **25**, pp. 1221-1230, 1992.
- [20] W.E. Forsyth, "Smithsonian Physical Tables," 9th Ed., Smithsonian Institution, Washington, D.C., 1954.
- [21] K.M. Armijo and J. Johnson, "Characterizing fire danger from low power PV arc faults," IEEE 40th Photovoltaics Specialists Conf., Denver, CO, 2014.
- [22] K. Samanta, M. Jassal, and A.K. Agrawal, "Atmospheric pressure glow discharge plasma and its applications in textile," *Indian J. Fibre & Textile Res.*, **31**, pp. 83-98, 2006.
- [23] A. Seidel, "Characterization and analysis of polymers," Wiley & Sons, New Jersey, 2008.
- [24] K.N. Pandiyaraj, V. Selvarajan and R.R. Deshmukh, "Effects of operating parameters on DC glow discharge plasma induced PET film surface," *J. of Phys. Conf. Series*, **208**, pp. 1-7, 2010.
- [25] T. Morimoto, T. Mori and S. Enomoto, "Ignition properties of polymers evaluated from ignition temperature and ignition limiting oxygen index," *J. App. Polymer Sci.*, **22**, pp. 1911-1918, 1978.
- [26] S. Carroccio, C. Puglisi and G. Montaudo, "Mechanisms of Thermal Oxidation of Poly(bisphenol A carbonate)" *Macromolecules*, **35**, p. 4297, 2002.
- [27] AC Plastics Inc., "Multiwall polycarbonate" *Material Safety Data Sheet*, Retrieved from: http://www.acplasticsinc.com/techsheets/UACI_140005_GL_Multiwall_MSDS_HR.pdf
- [28] A.D. Stokes and W.T. Oppenlander, "Electric arcs in open air," *J. Phys. D: Appl. Phys.*, **24**, pp. 26-35, 1991.
- [29] P. Zhu, J.J. Lowke and R. Morrow, "A unified theory of free burning arcs, cathode sheaths and cathodes," *J. Phys. D: Appl. Phys.*, **25**, pp. 1221-1230, 1992.
- [30] C.J. Luebke, T. Pier, B. Pahl, D. Breig and J. Zuercher, "Field Test Results of DC Arc Fault Detection on Residential and Utility Scale PV Arrays," 37th Photovoltaic Specialists Conference, Seattle, WA, 19-24 June 2011.
- [31] K.M. Armijo, J. Johnson, M. Hibbs, A. Fresquez, "Characterizing Fire Danger from Low Power PV Arc-Faults," 40th IEEE PVSC, Denver, CO, 8-13 June, 2014.
- [32] J. Johnson, K.M. Armijo, "Parametric Study of PV Arc-Fault Generation Methods and Analysis of Conducted DC Spectrum," 40th IEEE PVSC, Denver, CO, 8-13 June, 2014.
- [33] Wang, X. T., et al. "Optical spectroscopy of plasma produced by laser ablation of Ti alloy in air." *J. Applied physics*, **80**, No. 3, pp. 1783-1786, 1996.
- [34] F. P. Incropera, D. P. DeWitt, T. L. Bergman, A. S. Lavine, *Fundamentals of Heat and Mass Transfer*, 6th Ed. John Wiley & Sons, Inc., 2010.